Femtosecond Spectroscopy and Nonlinear Optical Properties of aza-BODIPY Derivatives in Solution

Hao-Jung Chang, Mykhailo V Bondar, Natalia Munera, Sylvain David, Olivier Maury, Gérard Berginc, Boris Le Guennic, Denis Jacquemin, Chantal Andraud, David J Hagan, et al.

10.1002/chem.202104072

WILEY-VCH

RESEARCH ARTICLE

Femtosecond spectroscopy and nonlinear optical properties of aza-BODIPY derivatives in solution

Hao-Jung Chang,[a] Mykhailo V. Bondar,[a,b] Natalia Munera,[a] Sylvain David,[c] Olivier Maury,[c] Gerard Berginc,[d] Boris Le Guennic,[e] Denis Jacquemin,[f] Chantal Andraud,[c] David J. Hagan,*[a] Eric W. Van Stryland[a]

[a] H. J. Chang, Dr. M. V. Bondar, Dr. N. Munera, Dr. D. J. Hagan, Dr. E. W. Van Stryland
CREOL, The Coloege of Optics and Photonics
University of Central Florida
Orlando, FL 32816 (USA)
E-mail: hagan@creol.ucf.edu
[b] Dr. M. V. Bondar
Institute of Physics NASU
Prospect Nauki, 46, Kyiv-28, 03028 (Ukraine)
[c] Dr. S. David, Dr. C. Andraud, Dr. O. Maury
Univ. Lyon, ENS Lyon, CNRS UMR 5182, Laboratoire de Chimie,
46 Allée d'Italie, 69364 Lyon, France
[d] Dr. G. Berginc
Thales LAS France
2 Avenue Gay Lussac, 78990 Élancourt (France)
[e] Dr. B. Le Guennic
CNRS, Institut des Sciences Chimiques de Rennes UMR 6266
Université Rennes
35000 Rennes (France)
[f] Dr. D. Jacquemin
CNRS, CEISAM UMR 6230
Univ. Nantes
44000 Nantes (France)

Supporting information for this article is given via a link at the end of the document.

Abstract: The fast relaxation processes in the excited electronic states of functionalized aza-boron-dipyrromethene (aza-BODIPY) derivatives (**1**-**4**) were investigated in liquid media at room temperature, including the linear photophysical, photochemical, and nonlinear optical (NLO) properties. Optical gain was revealed for nonfluorescent derivatives **3** and **4** in the near infrared (NIR) spectral range under femtosecond excitation. The values of two-photon absorption (2PA) and excited-state absorption (ESA) cross-sections were obtained for **1**-**4** in dichloromethane using femtosecond Z-scans, and the role of bromine substituents in the molecular structures of **2** and **4** is discussed. The nature of the excited states involved in electronic transitions of these dyes was investigated using quantum-chemical TD-DFT calculations, and the obtained spectral parameters are in reasonable agreement with the experimental data. Significant 2PA (maxima cross-sections ~ 2000 GM), and large ESA cross-sections ~ 10^{-20} m^2 of these new aza-BODIPY derivatives **1**-**4** along with their measured high photostability reveal their potential for photonic applications in general and optical limiting in particular.

Introduction

The development of new aza-boron-dipyrromethene (aza-BODIPY) molecular structures with specific linear photophysical and nonlinear optical (NLO) properties is a subject of great interest for photonics applications, including important multidisciplinary areas such as fluorescence biomaging,[1] photodynamic therapy,[2] organic photovoltaics,[3] etc. We highlight that NLO properties of aza-BODIPY derivatives[4] along with the fast excited-state charge-transfer phenomena[3b, 5] are promising for a number of practical applications related to 3D microfabrication, optical data storage,[6] optical signal processing[7] and optical power limiting (OPL) devices.[4a, 4b, 8] In fact, efficient broadband two-photon based OPL behavior was revealed for aza-BODIPY dyes in solution[4a, 8a] and solid-state glass matrix[4b] in the NIR spectral range up to telecommunication wavelengths, and the maximum values of two-photon absorption (2PA) cross-sections were obtained in the range of ≈ 3000 GM.[8a] The potential to enhance NIR-OPL properties of this molecular system using functionalized aza-BODIPY derivatives was demonstrated previously,[4a, 9] and the role of chemical modification of the aza-BODIPY core and peripheral moieties was comprehensively analyzed. Ultrafast photoinduced electron transfer and charge recombination processes were investigated in different aza-BODIPY derivatives covalently linked to fullerenes,[10] porphyrins,[11] phthalocyanines,[12] etc. using femtosecond transient absorption spectroscopy. For example, specific light-induced electron-transfer stages in the intramolecular relaxation processes allows optical gain in the system for certain wavelengths. The possibility to realize extremely fast energy transfer processes (~40 fs) in BODIPY-based oligomer structures was recently reported in ref.[13] as a potential mechanism for optoelectronic applications.

In this work NLO and fast relaxation processes in the electronic structure of aza-BODIPY derivatives **1**-**4** (see structures in Figure 1) were investigated by open aperture Z-

10.1002/chem.202104072

scans [14] and femtosecond transient absorption spectroscopy.[15] The effect of bromine atoms in the side positions of the aza-BODIPY core on the two-photon absorption (2PA), excited-state absorption (ESA), and characteristic times of the excited-state electronic relaxation was analyzed. The phenomenon of optical gain in the nonfluorescent aza-BODIPY derivatives was observed. Theoretical analysis of the electronic structure of **1**-**4** was performed based on TD-DFT quantum-chemical calculations.

Experimental Section

Synthetic procedures for 1-4

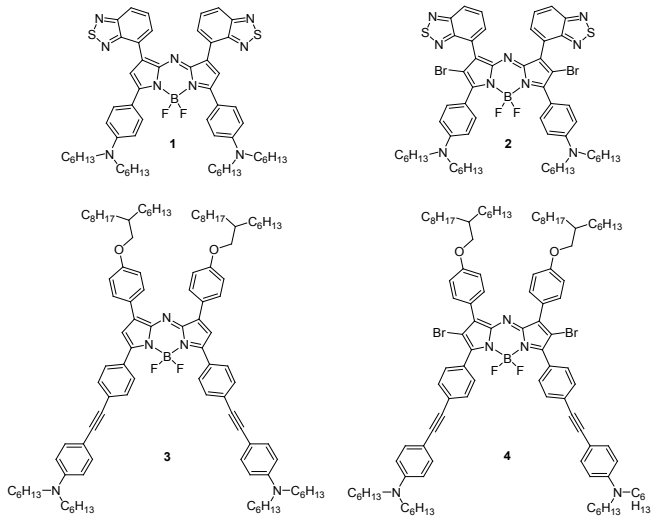

Figure 1. Structure of aza-BODIPY dyes **1**-**4**.

The study of 2PA and ESA dynamics were done on the four molecules **1**-**4** presented in Figure 1. The synthesis of the two precursors **1** and **3** was previously described in the ref.[16] za-BODIPY **1** is an analogue of a molecule recently described by Partridge et al.[17] where strong dihexylamine donors have been added in order to increase the donating effect and improve the solubility in organic solvents.[16a] Compound **3** is an analogue of a previously published aza-BODIPY dye,[4a] where solubility issues have been addressed by adding 1-decyl-2-hexyloxy chains on upper position.[16b] Twin molecules **2** and **4** are similar to, respectively, **1** and **3** but with two bromine atoms on the side pyrrolic positions. Halogenated aza-BODIPY molecules in these positions have been widely studied and numerous synthetic procedures for such compounds are presented in the literature.[18] It has been shown that halogenation of side positions was particularly efficient to induce intersystem crossing and favor triplet state population.[18b] Substitution with bromine atoms on molecules **2** and **4** was therefore believed to change the excited state dynamics. However, the described synthesis methods only concerned aza-BODIPY dyes bearing no or moderate donating groups and were hard to adapt to aza-BODIPY dyes bearing strong electron donating groups and/or alkyne moieties. Nowakowska et al.[19] had only very recently described molecules bearing strong amine donating groups and bromine atoms in side pyrrolic positions. Whereas bromination of **1** was readily achieved using classical *N*-bromosuccinimide (NBS) reagent, an alternative reactant, tetrabutylammonium tribromide ($TBABr_3$), was used to introduce halide atoms on these particular positions for compound **4** (scheme 1). Indeed, $TBABr_3$ was poorly reactive towards amine *ortho*-position and unreactive toward alkene bonds in acidic media. These qualities permitted obtaining molecule **4** in good yields after column chromatography purification (72%). Other synthetic details are presented in the Supporting Information.

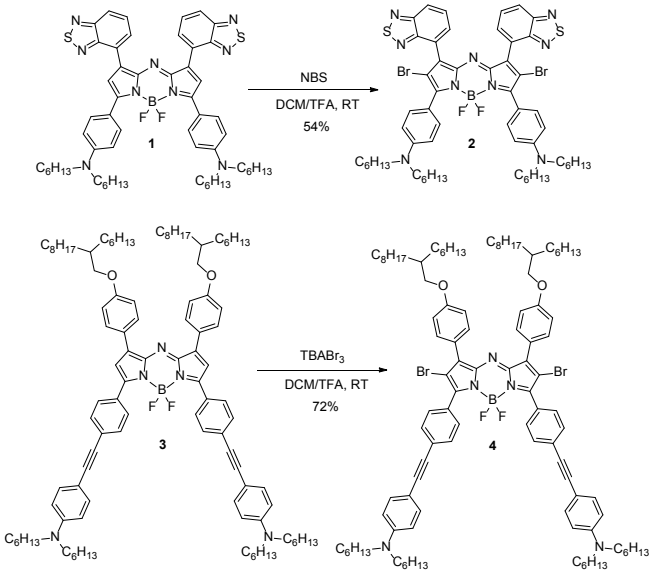

Scheme 1. Synthesis of aza-BODIPY dyes **2** and **4**.

Linear spectroscopy and photostability of 1-4

All linear spectroscopic and photochemical measurements of **1**-**4** were performed in air-saturated spectroscopic grade dichloromethane (DCM) at room temperature. The steady-state linear absorption (1PA) spectra of **1**-**4** were obtained in standard spectrophotometric 1 cm path length quartz cuvettes with a Varian Cary-500 spectrophotometer and dye concentrations, C ≈ 10^{-5} M. All fluorescence measurements were performed in dilute solutions (C ≈ 10^{-6} M) using a QuantaMaster spectrofluorometer (PTI, Inc.), 1 cm path length quartz cuvettes and corresponding spectral correction of the PTI detection system. The fluorescence quantum yields, Φ_{fl}, of **1**-**4** were determined by standard relative method,[20] using polymethine dye PD 2631 in ethanol as a reference.[21] The photochemical stability of **1**-**4** in air-saturated DCM was quantitatively estimated using the absorption method described previously in detail.[22] The values of photodecomposition quantum yields, Φ_{ph}, were obtained for continuous wave (CW) diode laser irradiation of the sample solutions at ≈ 635 nm with the average irradiance ≈ 500 mW/cm^2.

Z-scan and femtosecond transient absorption measurements

The degenerate 2PA and one-photon ESA cross-sections of **1-4** were determined in DCM at room temperature by open aperture Z-scans[14] using 1 mm path length quartz cuvettes with dye concentrations C ~ (1-6)·10^{-3} M. Z-scan measurements were performed with a regeneratively amplified Ti:sapphire laser (Clark MXR, CPA 2010; exit wavelength, 775 nm, pulse duration, τ_p ≈ 150 fs (FWHM), pulse energy, E_p ≈ 1 mJ, and repetition rate 1 kHz) which pumped an optical parametric amplifier (OPA, Light Conversion, TOPAS C) with a tuning range from 1100 nm – 2600 nm and energies up to ≈ 0.25 mJ. Focused spot sizes in the Z-scan setup were calibrated using Z-scans on a GaAs plate at each wavelength and the output pulse durations of the OPA were measured by the second-harmonic-generation autocorrelation technique.[23] Femtosecond transient absorption pump-probe measurements were realized with a Ti:Sapphire regenerative amplifier Legend Duo+ (Coherent, Inc.) with exit wavelength 800 nm, τ_p ≈ 40 fs, E_p ≈ 12 mJ, and a repetition rate of 1 kHz. The output of the Legend Duo+ at 800 nm was split in two parts. The first part was

10.1002/chem.202104072

focused into the sample solution and used as a pump beam. Investigated solutions were placed in 1 mm path length flow cells to avoid photodecomposition and thermo-optical distortion. The second part was focused into a 4 mm YAG crystal to generate a white light continuum (WLC) in the NIR spectral range,[24] filtered with 10 nm (FWHM) spike filters to extract specific probe wavelengths, λ_{pr}. The temporal resolution of the employed pump-probe setup was estimated as ≈ 300 fs, and other experimental details were described previously.[15, 25]

Computational details

We have used TD-DFT to probe the nature of the excited states involved in **1-4** in which the long alkyl chains were replaced by methyl groups during the calculations for the sake of saving computational time. We are well aware of the limitations of TD-DFT for (aza-)BODIPY dyes,[26] but the size of the compounds precludes the use of accurate wavefunction approaches. We have selected the CAM-B3LYP functional[27] for all our investigations. This functional includes long-range corrections and generally provides a good balance between local and charge-transfer excitations. First we have optimized the S_0 (DFT), S_1 (TD-DFT) and T_1 (U-DFT) with the 6-31G(d) basis set using the Gaussian16.A.03 program.[28] Default parameters have been used, except for tightened SCF (10^{-10}) and geometry (10^{-5}) convergence thresholds. Next, using the same program, we determined total and vertical 1PA transition energies using a much larger basis set, namely 6-311+G(2d,p), and accounting for solvent effects through the cLR[2] solvent model[29] that includes both linear-response and state-specific solvent corrections. Non-equilibrium solvation effects were accounted for. The ICT character of all states was characterized using the well-known Le Bahers' model.[30] The 2PA cross-sections were computed at the CAM-B3LYP/6-31G(d) level using the Dalton2016/2018 codes,[31] and selecting the S_0 geometry as obtained above. Default broadening functions have been applied. Eventually the spin-orbit coupling (SOC) elements between the singlet and triplet states have been determined with the latest Orca code[32] using the same functional and considering the TD-DFT S_1 minimum. We use the ZORA Hamiltonian, combined with *def2*-SVP basis set and the CPCM(SMD) solvent approach during the Orca calculations.

Results and Discussion

Linear photophysics and photostability

Table 1. Linear photophysical and photochemical parameters of **1-4** in DCM: steady-state absorption λ_{ab}^{max} and fluorescence λ_{fl}^{max} maxima, Stokes shifts, maximum extinction coefficients, ε^{max}, fluorescence quantum yields, Φ_{fl}, and photodecomposition quantum yields, Φ_{ph}.

Compound	**1**	**2**	**3**	**4**
λ_{ab}^{max}, nm	894 ± 1	873 ± 1	736 ± 1	700 ± 1
λ_{fl}^{max}, nm	963 ± 1	974 ± 1	-	-
Stokes shift, nm (cm^{-1})	69 ± 2 (1050)	101 ± 2 (1200)	-	-
ε^{max}, $10^3 M^{-1} \cdot cm^{-1}$	78 ± 4	21.5 ± 1	65 ± 3	49 ± 2
Φ_{fl}, %	1.7 ± 0.3	0.18 ± 0.04	-	-
Φ_{ph}, 10^{-8}	3.6	16	1	6

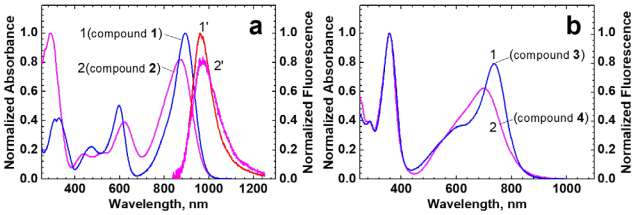

Figure 2. (a) Normalized 1PA (curves 1, 2) and corrected fluorescence (curves 1', 2') spectra of **1** and **2** in DCM. (b) Normalized 1PA spectra (1,2) for **3** (curve 1) and **4** (curve 2) in DCM.

The comparison of the steady-state 1PA spectra and main photophysical parameters of **1-4** in DCM (see Figure 2 and Table 1) reveals obvious effects of the bromine atoms in the aza-BODIPY core on the shape and corresponding spectral positions of the main long-wavelength absorption bands. Compounds **1** and **3** exhibit relatively sharp and intense 1PA bands (maximum extinction coefficients, ϵ^{max} ~ (65-78)·10^3 $M^{-1}cm^{-1}$), similar to symmetrical polymethine dyes in the spectral range 700 - 800 nm.[21] Aza-BODIPY derivatives with bromine atoms **2** and **4** are characterized by much broader absorption contours, noticeable decreases in the values of ε^{max}, and a blue shift of the absorption maximum with respect to that of non-brominated analogs, an effect related to the increase of twisting between the core of the dye and the lateral rings induced by the bulky halogen atoms, confirmed by theoretical calculations in the last part of the paper. The steady-state emission spectra were obtained for **1** and **2** in air-saturated DCM (Figure 2a, curves 1', 2') with relatively low fluorescence quantum yields, Φ_{fl} ≈ 1.7 % and 0.18 %, respectively. In contrast, fluorescence emission of **3** and **4** was undetectable ($\Phi_{fl} \leq 10^{-4}$) under the same experimental conditions. As follows from these data and from the transient absorption pump-probe measurements (see sec. 3.3), bromine atoms in the side positions of the aza-BODIPY chromophore noticeably decrease the values of the lowest electronic excited-state lifetimes of **2** and **4**, which can be assigned not only to the "heavy atom" effect and inter-system crossing towards triplet states (which is shown, below in the theoretical part, to be weak),[33] but also to the increase of twisting between the dye core and the lateral rings due to the halogen atoms, as mentioned above. It should be noticed that the obtained steady-state emission spectra of **1** and **2** were independent of the excitation wavelength, λ_{ex}, in the whole spectral range of linear absorption, and no violations of Kasha's rule[20] were observed.

Photostability of **1-4** was investigated in air-saturated DCM under CW diode laser irradiation at ≈ 635 nm using the absorption method,[22] and the obtained values of photodecomposition quantum yields, Φ_{ph}, are presented in Table 1. As follows from these data, all new compounds **1-4** exhibit relatively high levels of photostability (Φ_{ph} ~ 10^{-7} - 10^{-8}), that are comparable with the best laser dyes.[34] The first-order photoreaction was observed for **1-4** in DCM at room temperature, and bromine atoms in the molecular structures of **2** and **4** noticeably decrease their photochemical stability ≈ 4 and 6 times, respectively. It should be mentioned that even the lowest level of photostability, Φ_{ph} ≈ 1.6·10^{-7}, observed for **2**, remains applicable for a majority of optical applications.

10.1002/chem.202104072

2PA and ESA cross-sections

Table 2. Nonlinear absorption coefficients of **1**-**4** in DCM: 2PA cross-section, δ_{2PA}, in Göppert-Mayer (GM); one-photon ESA cross-section, σ_{ESA}, in 10^{-20} m^2

Wavelength, nm	Cross-section	Compound 1	2	3	4	
1150	δ_{2PA}	75 ± 20	70 ± 20	1370 ± 330	1990 ± 490	
	σ_{ESA}	7.1 ± 1.9	7.1 ± 0.9	0.3 ± 0.15	~ 0	
1200	δ_{2PA}	350 ± 60	155 ± 20	1900 ± 300	400 ± 70	
	σ_{ESA}	3.5 ± 0.8	0.35 ± 0.08	1.0 ± 0.2	3.5 ± 0.8	
1250	δ_{2PA}	90 ± 15	170 ± 25	750 ± 100	450 ± 85	
	σ_{ESA}	5 ± 0.8	0.1 ± 0.04	0.3 ± 0.08	0.2 ± 0.08	
1300	δ_{2PA}	95 ± 25	160 ± 25	620 ± 100	330 ± 60	
	σ_{ESA}	3.6 ± 1.3	0.05 ± 0.02	0.08 ± 0.03	0.3 ± 0.1	
1350	δ_{2PA}	80 ± 20	50 ± 15	460 ± 100	420 ± 70	
	σ_{ESA}	2.3 ± 0.6	0.45 ± 0.25	1.1 ± 0.3	~ 0	
1400	δ_{2PA}	50 ± 10	≤ 50	400 ± 70	640 ± 100	
	σ_{ESA}	0.5 ± 0.15	~ 0	0.34 ± 0.1	~ 0	
1500	δ_{2PA}	≤ 50	≤ 50	270 ± 50	250 ± 50	
	σ_{ESA}	~ 0	~ 0	~ 0	~ 0	
1550	δ_{2PA}	50 ± 10	55 ± 10	320 ± 60	360 ± 70	
	σ_{ESA}	0.85 ± 0.2	0.06 ± 0.02	1.75 ± 0.3	0.1 ± 0.05	
1700	δ_{2PA}	80 ± 20	65 ± 15	200 ± 40	260 ± 60	
	σ_{ESA}	~ 0	~ 0	~ 0	~ 0	

Nonlinear optical properties of **1**-**4** were investigated in the NIR spectral range (1150 – 1700 nm) using open aperture Z-scans [14] and some of the obtained experimental Z-scan curves with corresponding fits are presented in Figure 3. It should be mentioned that at the wavelengths of 1500 nm the best fits corresponded to purely 2PA (see Table 2). The change in the laser beam irradiance, I, due to nonlinear sample transmission is given by: $dI/dz = -\alpha_{2PA} \cdot I^2$ ($\alpha_{2PA} = (N_c/\hbar\omega) \cdot \delta_{2PA}$ is the 2PA

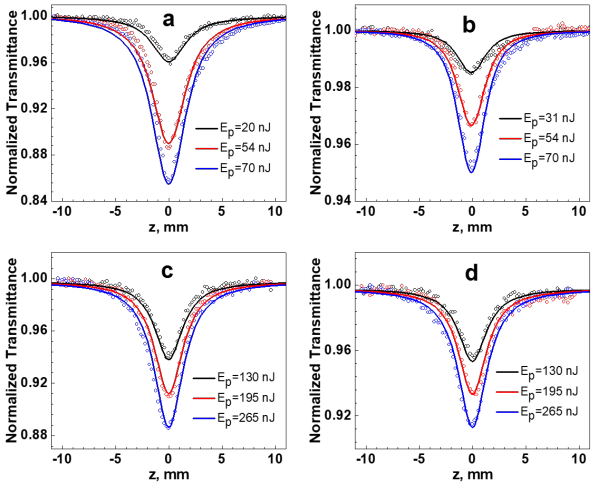

Figure 3. Open aperture Z-scans (separate points) and fittings curves (solid lines) for corresponding pulse energies, obtained for **3** (a, c) and **4** (b, d) in DCM at 1200 nm (a, b) and 1500 nm (c, d).

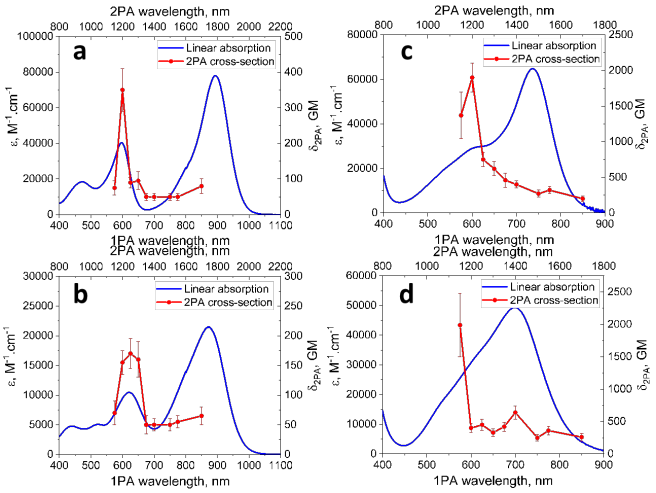

Figure 4. Molar absorptivity and 2PA cross section spectra for **1** (a) and **3** (c) and brominated counterparts **2** (b) and **4** (d) in DCM.

coefficient, N_c, $\hbar\omega$, δ_{2PA}, and z are the sample concentration, photon energy, 2PA cross-section and propagation axis, respectively). In contrast, corresponding changes in the beam irradiance at the other wavelengths cannot be completely described solely by 2PA but can be described by 2PA plus ESA: $dI/dz = -\alpha_{2PA} \cdot I^2 - \sigma_{ESA} \cdot N(I) \cdot I$, where $N(I)$ is the population density in the first excited state and σ_{ESA} is the one-photon ESA cross-section.[4c] The obtained values of δ_{2PA} and σ_{ESA} for **1**-**4** in DCM are presented in Table 2. One-photon absorption and degenerate 2PA spectra for **1**-**4** in DCM are shown in Figure 4. For comparison of transition wavelength, spectra are shown on the same graph with separate axes for one-photon absorption (bottom) and 2PA (top) wavelength. As follows from these data, the shape, spectral position, and maxima values of the 2PA spectra remain nearly the same for **1** and **2**. Compounds **3** and **4** exhibit much broader linear absorption contours with complicated electronic nature (see quantum-chemical analysis in sec. 3.4), and noticeable differences between their 2PA spectra. Relatively strong 2PA peaks were observed for **3** at 1200 nm (Figure 4c),

10.1002/chem.202104072

and for **4** at ~ 1150 nm (Figure 4d) that can be related to higher excited electronic levels.

The majority of the obtained values of σ_{ESA} were systematically larger for **1** in comparison with its brominated counterparts **2** (Table 2). It is worth mentioning that the values of σ_{ESA} for **1** and **4** at 1200 nm exceed the corresponding ground state 1PA cross-section maxima by 1.2 and 1.9 times, respectively. It should be mentioned that new aza-BODIPY derivatives exhibit much higher 2PA cross-sections in the telecommunication spectral range than methoxy and hydroxy substituted aza-BODIPYs (< 15 GM)[35] and BF_2-azadipirromethenes (< 2 GM),[36] and therefore, possess high potential for practical applications.

Femtosecond transient absorption spectroscopy

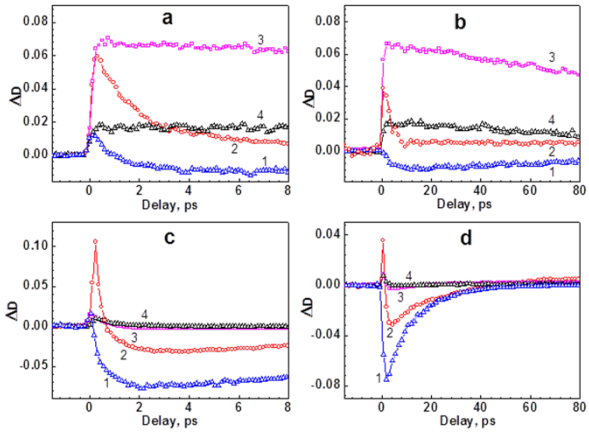

Figure 5. Typical kinetic dependences $\Delta D(\tau_D)$ for **1** (a, b) and **2** (c, d) in DCM under excitation at 800 nm: λ_{pr} = 1000 nm (1), 1020 nm (2), 1140 nm (3), and 1350 nm (4). Femtosecond (a, c) and picosecond (b, d) resolution.

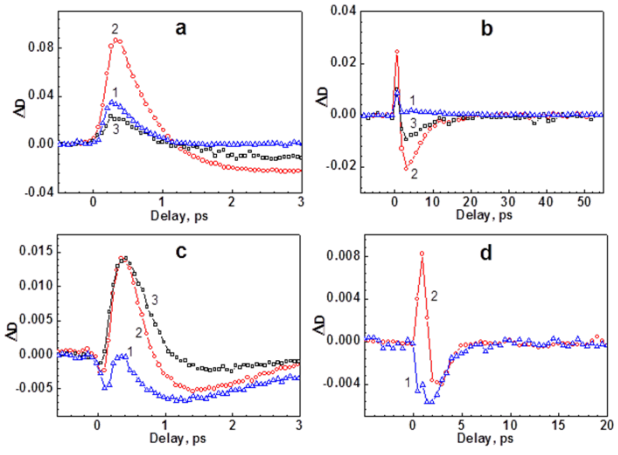

Figure 6. Typical kinetic dependences $\Delta D(\tau_D)$ for **3** (a, b) and **4** (c, d) in DCM under excitation at 800 nm: (a, b) λ_{pr}= 1100 nm (1), 1200 nm (2), and 1300 nm (3); (c, d) λ_{pr}= 1000 nm (1), 1100 nm (2), and 1200 nm (3). Femtosecond (a, c) and picosecond (b, d) resolution.

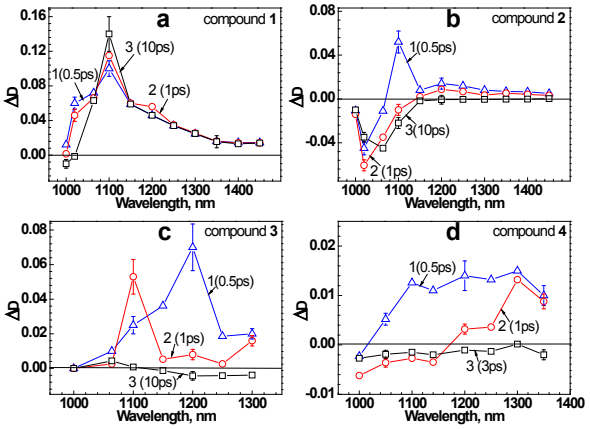

Figure 7. Time-resolved ESA spectra of **1** (a), **2** (b), **3** (c), and **4** (d) in DCM: (a, b, c) τ_D= 0.5 ps (1), 1 ps (2), and 10 ps (3); (d) τ_D= 0.5 ps (1), 1 ps (2), and 3 ps (3).

Fast relaxation processes in the excited electronic states of **1**-**4** in DCM were investigated at room temperature by transient absorption pump-probe experiments[15, 25] in the broad NIR spectral range for excitation (pump) wavelength at 800 nm. Typical kinetic dependences of the induced optical density, $\Delta D = \log(1/T)$ on the temporal delay between pump and probe pulses, τ_D, are shown in Figure 5 and Figure 6 for specific probe wavelengths, λ_{pr}. Both positive and negative values of ΔD are observed for all the compounds investigated. Considering that all probe wavelengths (λ_{pr} ≥1000 nm) were in the spectral range of negligible ground-state absorption of **3** and **4** (see Figure 2) we conclude that one-photon (800 nm) initiated ESA processes dominate (positive ΔD) and note optical gain phenomena (negative ΔD) in the range without linear absorption. For **1** and **2** (see Figure 5), we see similar results except in the range between 1000 nm and 1050 nm where additional ground-state saturable absorption can take place. It should be mentioned that compounds **3** and **4** exhibit no fluorescence emission ($\Phi_{fl} < 10^{-4}$) and optical gain looks strange in this case of extremely fast nonradiative transition $S_1 \rightarrow S_0$ (see "spikes" followed by ps relaxation processes in Figure 4c, d). In general, optical gain for nonfluorescent light-absorbing organic compounds was reported previously by Min *et al.*,[37] where their stimulated emission processes were realized under high intensity laser irradiation for stimulated emission microscopy imaging. In our case, optical gain was observed for **1** (at 10 ps, 1000 nm), **2** (at 2 ps, 1000 nm), **3** (at 3 ps, 1200 nm), and **4** (at 1 ps, 1100 nm). The largest values of negative ΔD were obtained for brominated derivative **2** in the spectral range 1000 - 1150 nm (transmission increases around 8% at 2 ps, 1000 nm) and non-brominated **3** in the spectral range 1000 - 1200 nm (transmission increases 5% at 3 ps, 1200 nm) under the same excitation conditions. It is important to note that the maximum possible loss in these spectral regions was less than 1%. Long temporal components of the ESA kinetic signals from weakly fluorescent **1** and **2** (Figure 5b, d) are correlated with corresponding values of the fluorescence quantum yields (see Table 1), and presumably, can be assigned to the lowest electronic excited-state lifetimes. It is worth mentioning that the

10.1002/chem.202104072

bromination of **1** leads to a dramatic decrease in the Φ_{fl} and lifetime of S_1. Negative values of ΔD are evidence of population inversion between S_1 and S_0 vibronic levels which arises in the first several picoseconds (Figure 5a, 5c, Figure 6a, 6c) after relaxation of the intense positive ESA signal possibly related to Franck-Condon and/or solvate reorganization processes.[20] Time-resolved ESA spectra of **1**-**4** were obtained from the corresponding transient absorption kinetic curves and are shown in Figure 7 for specific time delays, τ_D. As follows from these data, the strongest negative ΔD signals were observed for **2** (Figure 7b) (the probe transmission at 1020nm increase by 17% at 1 ps delay after the pump) in the spectral range of its fluorescence contour 1000 - 1200 nm (Figure 2a). A complicated temporal behavior of the positive ESA bands was revealed for **2** at ≈ 1100 nm (Figure 7b), and in the range of 1100 nm - 1300 nm for **3** and **4** (Figure 7c, d). These relatively fast (~ 0.5-1 ps) and complicated processes can be related to intramolecular photoinduced electron transfer (PET) phenomena[38] typically proposed for the description of fluorescence quenching mechanisms in amino-functionalized aza-BODIPY derivatives.[8a, 39]

Obtained data on time-resolved ESA spectra of **1**-**4** in combination with the 2PA cross-section values (see Table 2) reveal their potential for applications such as OPL in the NIR spectral range.[8a]

Quantum-chemical analysis of the electronic structure

To complete the experimental studies, theoretical calculations have been performed and several conclusions emerge. The main results are summarized in Figure 8. First, the ground-state geometries are substantially perturbed by the presence of the lateral bromine atoms. For instance, in **1**, the dihedral angle between the upper benzothidiazole groups and the aza-BODIPY core is 19°, whereas the steric effect makes this angle much larger in **2**, 48°. In going from **3** to **4**, the corresponding dihedral angle between the *p*-methoxy-phenyl and the aza-BODIPY core also increases substantially from 25° to 37°. These large geometrical differences qualitatively explain the differences of band shapes and of the excited state positions obtained for the brominated and non-brominated compounds. Indeed, as can be seen in Figure 8, the bromination does not significantly affect the oscillator strength nor the nature of the lowest excited state. In fact, the electron density difference (EDD) plots reveal that this lowest state is always mainly centered on the aza-BODIPY (with no contribution on the bromine), except for a moderate ICT character from the lower amino groups in both **1** and **2** (that have CT distance of ca. 2.5 Å). This lowest transition presents a large 1PA oscillator strength, and modest 2PA cross sections in the 50-100 GM range, due to the moderate ICT character of this transition. This S_0-S_1 transition corresponds to the most redshifted absorption in the experimental spectra of Figure 4, and the values listed in Figure 8 reproduce the experimental trends, *i.e.*, the redshifts go from largest to smallest as **1** > **2** > **3** > **4** (see Table 1). The fact that the theoretical values are blueshifted is explainable by the vertical approximation. Indeed we have computed the corresponding 0-0 wavelength for **1**: 903 nm. This value can be straightforwardly compared to the absorption/fluorescence crossing: 930 nm, hinting that the selected level of theory is sufficient for our purposes.

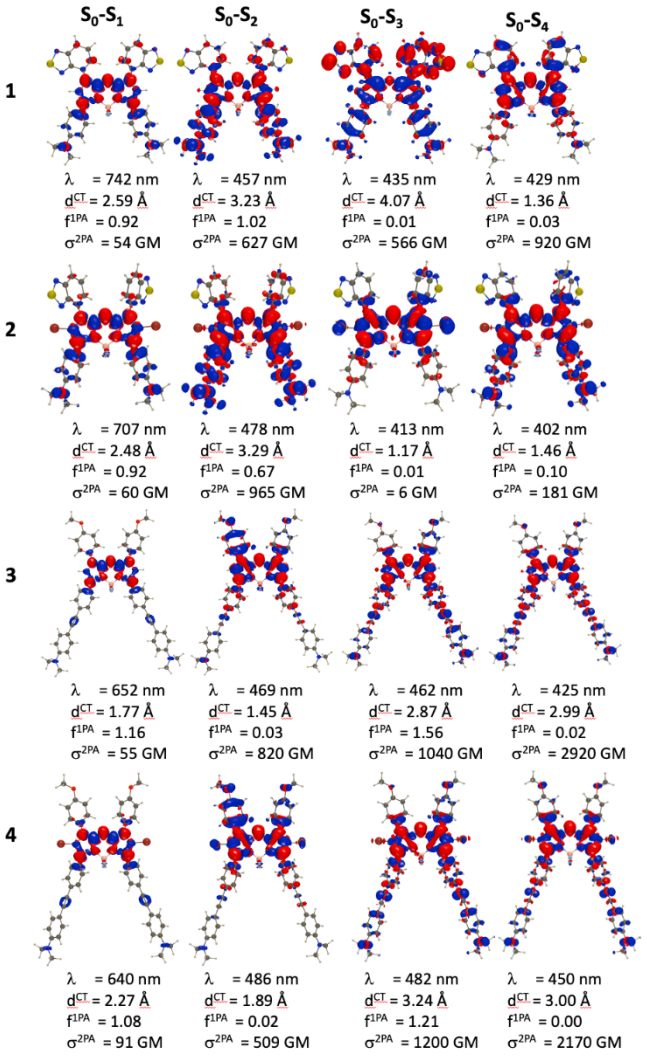

Figure 8. Representation of the density difference plots for the four lowest vertical transitions in all compounds. The blue and red lobes indicate decrease and increase of density upon excitation. For each state, we report the vertical absorption wavelength, and the corresponding CT distances, oscillator strength and 2PA cross-section, as computed by theory.

In both **1** and **2**, the second transition is significantly allowed in both one and two photon processes, with large ICT from the lower part to the aza-BODIPY core. The large computed responses of several hundreds of GM indicate that the strong response of ca. 210 - 280 GM found around 1200 - 1250 nm in the experimental spectra of Figure 4a,b are indeed originating from the S_0-S_2 transition. Again, computations give too blushifted transitions due to the use of the vertical approximation. At this stage, it is noteworthy that for the third excited state, not explored experimentally, there is a significant topological difference between **1** and **2**: for both molecules the S_0-S_3 excitation leads to a local state with a trifling 1PA response , and a high 2PA efficiency for **1,** which could be due to the contribution of transition

dipole moments between excited states, while for **2**, this transition is the first to significantly involve the bromine atom which is detrimental for its 2PA response.

Let us now turn towards **3** and **4**. It is interesting to note that their S_1 state is significantly blueshifted as compared to **1** and **2**, whereas the position of the S_2 transition is mostly unchanged and S_3 appears at almost the same energy as S_2, whereas the separation was much clearer in the two first dyes. This likely explains the very broad band linear absorption obtained experimentally for **3** and **4** (Figure 4c,d, blue curves). They actually engulf several electronic transitions. In both **3** and **4**, the EDD reveals that the second transition corresponds to a mild ICT from one of the top *p*-methoxy-phenyl to the core of the aza-BODIPY, whereas the third excitation involves a long-range ICT from the bottom amino groups. The total 2PA cross sections determined for those two transitions are similar in **3** (1900 GM) and **4** (1990 GM), and are clearly significantly larger than the corresponding response of the second excited state in **1** and **2**. These total 2PA cross sections are qualitatively well in line with the experimental trends of a strong response of ~ 2000 GM in the large "shoulder" at ~ 600 nm (Figure 4).

Finally, given the presence of bromine atoms, we have investigated the intersystem-crossing (ISC). As usual in such process, the dominating pathway should be first a geometrical relaxation to the S_1 before ISC. Therefore, we have computed the position of the triplets at this optimal S_1 geometry. In all dyes, TDA-DFT returns only one triplet (T_1) below S_1, indicating that ISC to higher lying triplets is highly unlikely. The spin-orbit coupling elements corresponding to this S_1-T_1 ISC process indicates, as expected, totally negligible coupling in both **1** (0.03 cm^{-1}) and **3** (0.01 cm^{-1}) and becomes larger, but yet not impressive, in the brominated structures, i.e., **2** (0.65 cm^{-1}) and **4** (1.67 cm^{-1}). These latter values are compatible with a slow ISC, and their moderate magnitude is the logical consequence of the rather passive role of the bromine atoms in the S_1 state. Using U-DFT, we computed 0-0 phosphorescence at 0.68 eV and 0.73 eV for **2** and **4**, respectively. These tiny values indicate that the non-radiative pathway strongly dominates once in T_1. These values are also too small to allow the formation of singlet oxygen.

Conclusion

The steady-state photophysical parameters, photochemical stability, NLO properties and fast relaxation in the excited electronic states of these new aza-BODIPY derivatives **1**-**4** were investigated in DCM at room temperature. Bromination of **1** and **3** resulted in a noticeable broadening of the 1PA absorption band, substantial decrease in the values of ε^{max}, Φ_{fl}, lifetimes of the first excited state, and photochemical stability. The largest 2PA cross-sections of **1**-**4** (around 2000 GM) were obtained at 1200 nm for **3** and at 1150 nm for **4**. The introduction of bromine substituents in the side position of the aza-BODIPY core leads to change in the shape of δ_{2PA} spectra. The largest additional absorption from 2PA initiated ESA was detected for **1**-**4** between 1150 nm and 1250 nm and corresponding values of σ_{ESA} were in the range (1-7)·10^{-20} m^2. The investigation of fast relaxation processes in the excited states of **1**-**4** reveals the unusual phenomenon of optical gain for nonfluorescent compounds **3** and **4** which was observed on the time scale of several picoseconds after the excitation. The time-resolved ESA spectra exhibit complicated temporal behavior with the main ESA bands arising in the first 0.5 - 1 ps in the NIR spectral range 1100 - 1300 nm.

Quantum chemical calculations of the main electronic parameters of new aza-BODIPY derivatives were performed at the TD/DFT level of theory and helped rationalize the different 1PA and 2PA responses obtained experimentally.

Linear spectroscopic properties and high photostability, NIR 2PA and ESA cross-sections, and specific fast relaxation processes in the excited electronic states of aza-BODIPYs **1**-**4** reveal their potential for applications in photonic devices.

Acknowledgements

EVS and DJH thank the Army Research Lab (W911NF-15-2-0090) for support. MVB wishes to thank the National Academy of Sciences of Ukraine (VC/188, and V-204). CA and OM thank Thales LAS for financial support and for the grant of SD. DJ is indebted to Dr. Le Bahers (Lyon) for fruitful discussions. We thank the CCIPL computational center in Nantes for generous allocation of computational time.

Keywords: aza-boron dipyrromethene derivatives • femtosecond transient absorption pump-probe spectroscopy • two-photon absorption • TD-DFT calculations.

[1] a) D. Wu, S. Cheung, G. Sampedro, Z.-L. Chen, R. A. Cahill, D. F. O'Shea, *Biomembranes* **2018**, *1860*, 2272-2280; b) W. Sheng, J. Cui, Z. Ruan, L. Yan, Q. Wu, C. Yu, Y. Wei, E. Hao, L. Jiao, *J. Org. Chem.* **2017**, *82*, 10341-10349; c) A. Kamkaew, S. Thavornpradit, T. Puangsamlee, D. Xin, N. Wanichacheva, K. Burgess, *Org. Biomol. Chem.* **2015**, *13*, 8271-8276; d) M. Grossi, M. Morgunova, S. Cheung, D. Scholz, E. Conroy, M. Terrile, A. Panarella, J. C. Simpson, W. M. Gallagher, D. F. O'Shea, *Nat. Commun.* **2016**, *7*, 10855/10851-10813; e) J. Pliquett, A. Dubois, C. Racoeur, N. Mabrouk, S. Amor, R. Lescure, A. Bettaïeb, B. Collin, C. Bernhard, F. Denat, P. S. Bellaye, C. Paul, E. Bodio, C. Goze, *Bioconjugate Chem.* **2019**, *30*, 1061-1066; f) M. H. Y. Cheng, K. M. Harmatys, D. M. Charron, J. Chen, G. Zheng, *Angew. Chem. Int. Ed. Engl.* **2019**, *58*, 13394-13399.

[2] a) A. T. Byrne, A. E. O'Connor, M. Hall, J. Murtagh, K. O'Neill, K. M. Curran, K. Mongrain, J. A. Rousseau, R. Lecomte, S. McGee, J. J. Callanan, D. F. O'Shea, W. M. Gallagher, *Br. J. Cancer* **2009**, *101*, 1565-1573; b) V. Ibrahimova, S. A. Denisov, K. Vanvarenberg, P. Verwilst, V. Préat, J.-M. Guigner, N. D. McClenaghan, S. Lecommandoux, C.-A. Fustin, *Nanoscale* **2017**, *9*, 11180-11186; c) A. E. O'Connor, M. M. Mc Gee, Y. Likar, V. Ponomarev, J. J. Callanan, D. F. O'shea, A. T. Byrne, W. M. Gallagher, *Int. J. Cancer* **2012**, *130*, 705-715; d) Y. Zhang, S. Bo, T. Feng, X. Qin, Y. Wan, S. Jiang, C. Li, J. Lin, T. Wang, X. Zhou, Z. X. Jiang, P. Huang, *Adv. Mater.* **2019**, *32*, e1806444; e) N. Adarsh, P. S. S. Babu, R. R. Avirah, M. Viji, S. A. Nair, D. Ramaiah, *J. Mater. Chem. B* **2019**, *2019*, 2372-2377; f) Q. Wang, D. K. P. Ng, P.-C. Lo, *J. Mater. Chem. B* **2018**, 3285-3296; g) Ł. Łapok, I. Cieślar, T. Pędziński, K. M. Stadnicka, M. Nowakowska, *ChemPhysChem* **2020**, *21*, 725-740; h) P. C. A. Swamy, G. Sivaraman, R. N. Priyanka, S. O. Raja, K. Ponnuvel, J. Shanmugpriya, A. Gulyani, *Coord. Chem. Rev.* **2020**, *411*, 213233.

[3] a) W. Senevirathna, J.-Y. Liao, Z. Mao, J. Gu, M. Porter, C. Wang, R. Fernando, G. Sauve, *J. Mater. Chem. A* **2015**, *3*, 4203-4214; b) K. Flavin, K. Lawrence, J. Bartelmess, M. Tasior, C. Navio, C. Bittencourt, D. F. O'Shea, D. M. Guldi, S. Giordani, *ACS Nano* **2011**, *5*, 1198-1206; c) W. Sheng, Y.-Q. Zheng, Q. Wu, Y. Wu, C. Yu, L. Jiao, E. Hao, J.-Y. Wang, J. Pei, *Org. Lett.* **2017**, *19*, 2893-2896; d) R. Feng, N. Sato, T. Yasuda, H. Furuta, S. Shimizu, *Chem. Commun.* **2020**, *56*, 2975-2978.

[4] a) P.-A. Bouit, K. Kamada, P. Feneyrou, G. Berginc, L. Toupet, O. Maury, C. Andraud, *Adv. Mater.* **2009**, *21*, 1151-1154; b) D. Chateau, Q. Bellier, F. Chaput, P. Feneyrou, G. Berginc, O. Maury, C. Andraud, S. Parola, *J. Mater. Chem. C* **2014**, *2*, 5105-5110; c) Q. Bellier, N. S.

Makarov, P.-A. Bouit, S. Rigaut, K. Kamada, P. Feneyrou, G. Berginc, O. Maury, J. W. Perry, C. Andraud, *Phys. Chem. Chem. Phys., 2012, 14, 15299–15307* **2012**, *14*, 15299-15307.

[5] a) V. Bandi, M. E. El-Khouly, V. N. Nesterov, P. A. Karr, S. Fukuzumi, F. D'Souza, *J. Phys. Chem. C* **2013**, *117*, 5638-5649; b) A. N. Amin, M. E. El-Khouly, N. K. Subbaiyan, M. E. Zandler, S. Fukuzumi, F. D'Souza, *Chem. Commun.* **2012**, *48*, 206-208.

[6] a) I. Wang, M. Bouriau, P. L. Baldeck, C. Martineau, C. Andraud, *Opt. Lett.* **2002**, *27*, 1348-1350; b) K.-S. Lee, D.-Y. Yang, S. H. Park, R. H. Kim, *Polym. Adv. Technol.* **2006**, *17*, 72-82; c) S. Kawata, H.-B. Sun, T. Tanaka, K. Takada, *Nature* **2001**, *412*, 697-698.

[7] a) J. M. Hales, S. Barlow, H. Kim, S. Mukhopadhyay, J.-L. Brédas, J. W. Perry, S. R. Marder, *Chem. Mater.* **2014**, *26*, 549-560; b) T. Gao, W. Que, J. Shao, Y. Wang, *J. Appl. Phys.* **2015**, *118*, 155502/155501-155502/155506. .

[8] a) S. Pascal, Q. Bellier, S. David, P.-A. Bouit, S.-H. Chi, N. S. Makarov, B. L. Guennic, S. Chibani, G. Berginc, P. Feneyrou, D. Jacquemin, J. W. Perry, O. Maury, C. Andraud, *J. Phys. Chem. C* **2019**, *123*, 23661-23673; b) S. David, D. Chateau, H.-J. Chang, L. H. Karlsson, M. V. Bondar, C. Lopes, B. Le Guennic, D. Jacquemin, G. Berginc, O. Maury, S. Parola, C. Andraud, *J. Phys. Chem. C* **2020**, *124*, 24344-24350.

[9] X. Liu, J. Zhang, K. Li, X. Sun, Z. Wu, A. Ren, J. Feng, *Phys. Chem. Chem. Phys.* **2013**, *15*, 4666-4676.

[10] a) V. Bandi, M. E. El-Khouly, K. Ohkubo, V. N. Nesterov, M. E. Zandler, S. Fukuzumi, F. D'Souza, *J. Phys. Chem. C* **2014**, *118*, 2321-2332; b) V. Bandi, F. P. D'Souza, H. B. Gobeze, F. D'Souza, *Chem. Eur. J.* **2015**, *21*, 2669-2679.

[11] a) V. Bandi, K. Ohkubo, S. Fukuzumi, F. D'Souza, *Chem. Commun.* **2013**, *49*, 2867-2869; b) V. Bandi, H. B. Gobeze, P. A. Karr, F. D'Souza, *J. Phys. Chem. C* **2014**, *118*, 18969-18982.

[12] H. B. Gobeze, V. Bandi, F. D'Souza, *Phys. Chem. Chem. Phys.* **2014**, *16*, 18720-18728.

[13] L. J. Patalag, J. Hoche, M. Holzapfel, A. Schmiedel, R. Mitric, C. Lambert, D. B. Werz, *J. Am. Chem. Soc.* **2021**, *143*, 7414-7425.

[14] M. Sheik-Bahae, A. A. Said, T. H. Wei, D. J. Hagan, E. W. Van Stryland, *IEEE J. Quantum Elect.* **1990**, *26*, 760-769.

[15] P. Zhao, S. Tofighi, R. M. O'Donnell, J. Shi, P. Y. Zavalij, M. V. Bondar, D. J. Hagan, E. W. Van Stryland, *J. Phys. Chem. C* **2017**, *121*, 23609-23617.

[16] a) S. David, H.-J. Chang, C. Lopes, C. Brännlund, B. Le Guennic, G. Berginc, E. Van Stryland, M. V. Bondar, D. Hagan, D. Jacquemin, C. Andraud, O. Maury, *Chem. Eur. J.* **2021**, *27*, 3517-3525; b) S. David, G. Pilet, G. Berginc, C. Andraud, O. Maury, *New Journal of Chemistry* **2020**, *44*, 13125-13130.

[17] E. M. A. Al-Imarah, P. J. Derrick, A. Partridge, *Journal of Photochemistry and Photobiology A: Chemistry* **2017**, *337*, 82-90.

[18] a) A. Gorman, J. Killoran, C. O'Shea, T. Kenna, W. M. Gallagher, D. F. O'Shea, *J. Am. Chem. Soc.* **2004**, *126*, 10619-10631; b) N. Adarsh, M. Shanmugasundaram, R. R. Avirah, D. Ramaiah, *Chem. Eur. J.* **2012**, *18*, 12655-12662 ; cA. Karataya, M. C. Miser, X. Cui, B. Küçüköz, H. Yılmaz, G. Sevinç, E. Akhüseyin, X. Wu, M. Hayvali, H. G. Yaglioglu, J. Zhao, A. Elmali, *Dyes Pigm.* **2015**, *122*, 286-294.

[19] M. Obłoza, Ł. Łapok, T. Pędziński, K. M. Stadnicka, M. Nowakowska, *ChemPhysChem* **2019**, *20*, 2482-2497.

[20] J. R. Lakowicz, *Principles of fluorescence spectroscopy*, Kluwer, New York, **1999**.

[21] S. Webster, L. A. Padilha, H. Hu, O. V. Przhonska, D. J. Hagan, E. W. Van Stryland, M. V. Bondar, I. G. Davydenko, Y. L. Slominsky, A. D. Kachkovski, *J. Lumin.* **2008**, *128*, 1927-1936.

[22] C. C. Corredor, K. D. Belfield, M. V. Bondar, O. V. Przhonska, S. Yao, *J. Photoch. Photobio. A* **2006**, *184*, 105-112.

[23] C. Rulliere, *Femtosecond laser pulses: principles and experiments*, 2nd ed., Springer Science+Business Media, Inc., **2005**.

[24] M. Bradler, ;, P. Baum, E. Riedle, *Appl. Phys. B* **2009**, *97*, 561-574.

[25] T. Liu, M. V. Bondar, K. D. Belfield, D. Anderson, A. E. Masunov, D. J. Hagan, E. W. Van Stryland, *J. Phys. Chem. C* **2016**, *120*, 11099-11110.

[26] a) S. Chibani, A. D. Laurent, B. Le Guennic, D. Jacquemin, *J. Chem. Theory Comput.* **2014**, *10*, 4574-4582; b) B. Le Guennic, D. Jacquemin, *Acc. Chem. Res.* **2015**, *48*, 530-537.

[27] T. Yanai, D. P. Tew, N. C. Handy, *Chem. Phys. Lett.* **2004**, *393*, 51-57.

[28] M. J. Frisch, G. W. Trucks, H. B. Schlegel, G. E. Scuseria, M. A. Robb, J. R. Cheeseman, G. Scalmani, V. Barone, B. Mennucci, G. A. Petersson, H. Nakatsuji, M. Caricato, X. Li, H. P. Hratchian, A. F. Izmaylov, J. Bloino, G. Zheng, J. L. Sonnenberg, M. Hada, M. Ehara, K. Toyota, R. Fukuda, J. Hasegawa, M. Ishida, T. Nakajima, Y. Honda, O. Kitao, H. Nakai, T. Vreven, J. J. A. Montgomery, J. E. Peralta, F. Ogliaro, M. Bearpark, J. J. Heyd, E. Brothers, K. N. Kudin, V. N. Staroverov, R. Kobayashi, J. Normand, K. Raghavachari, A. Rendell, J. C. Burant, S. S. Iyengar, J. Tomasi, M. Cossi, N. Rega, N. J. Millam, M. Klene, J. E. Knox, J. B. Cross, V. Bakken, C. Adamo, J. Jaramillo, R. Gomperts, R. E. Stratmann, O. Yazyev, A. J. Austin, R. Cammi, C. Pomelli, J. W. Ochterski, R. L. Martin, K. Morokuma, V. G. Zakrzewski, G. A. Voth, P. Salvador, J. J. Dannenberg, S. Dapprich, A. D. Daniels, Ö. Farkas, J. B. Foresman, J. V. Ortiz, J. Cioslowski, D. J. Fox, C. Wallingford, Gaussian, Inc., Wallingford CT, **20016**.

[29] P. M. Vérité, C. A. Guido, D. Jacquemin, *Phys. Chem. Chem. Phys.* **2019**, *21*, 2307-2317.

[30] a) T. Le Bahers, C. Adamo, I. Ciofini, *J. Chem. Theory Comput.* **2011**, *7*, 2498-2506; b) D. Jacquemin, T. Le Bahers, C. Adamo, I. Ciofini, *Phys. Chem. Chem. Phys.* **2012**, *14*, 5383-5388.

[31] K. Aidas, C. Angeli, K. L. Bak, V. Bakken, R. Bast, L. Boman, O. Christiansen, R. Cimiraglia, S. Coriani, P. Dahle, E. K. Dalskov, U. Ekström, T. Enevoldsen, J. J. Eriksen, P. Ettenhuber, B. Fernández, L. Ferrighi, H. Fliegl, L. Frediani, K. Hald, A. Halkier, C. Hättig, H. Heiberg, T. Helgaker, A. C. Hennum, H. Hettema, E. Hjertenæs, S. Høst, I.-M. Høyvik, M. F. Iozzi, B. Jansik, H. J. A. Jensen, D. Jonsson, P. Jørgensen, J. Kauczor, S. Kirpekar, T. Kjærgaard, W. Klopper, S. Knecht, R. Kobayashi, H. Koch, J. Kongsted, A. Krapp, K. Kristensen, A. Ligabue, O. B. Lutnæs, J. I. Melo, K. V. Mikkelsen, R. H. Myhre, C. Neiss, C. B. Nielsen, P. Norman, J. Olsen, J. M. H. Olsen, A. Osted, M. J. Packer, F. Pawlowski, T. B. Pedersen, P. F. Provasi, S. Reine, Z. Rinkevicius, T. A. Ruden, K. Ruud, V. Rybkin, P. Salek, C. C. M. Samson, A. S. de Merás, T. Saue, S. P. A. Sauer, B. Schimmelpfennig, K. Sneskov, A. H. Steindal, K. O. Sylvester-Hvid, P. R. Taylor, A. M. Teale, E. I. Tellgren, D. P. Tew, A. J. Thorvaldsen, L. Thøgersen, O. Vahtras, M. A. Watson, D. J. D. Wilson, M. Ziolkowski, H. Ågren, *WIREs Comput. Mol. Sci.* **2014**, *4*, 269-284.

[32] F. Neese, *WIREs Comput. Mol. Sci.* **2018**, *8*, e1328/1321-1326.

[33] S. K. Lower, M. A. El-Sayed, *Chem. Rev.* **1966**, *66*, 199-241.

[34] a) I. Rosenthal, *Opt. Commun.* **1978**, *24*, 164-166; b) S. A. El-Daly, S. A. El-Azim, F. M. Elmekawey, B. Y. Elbaradei, S. A. Shama, A. M. Asiri, *Int. J. Photoenergy* **2012**, *2012*, 458126/458121-458110; c) S. A. Azim, S. M. Al-Hazmy, E. M. Ebeid, S. A. El-Daly, *Opt. Laser Technol.* **2005**, *37*, 245-249.

[35] B. Kücüköz, M. Hayvalı, H. Yılmaz, B. Uguz, U. Kürüm, H. G. Yaglioglu, A. Elmali, *J. Photoch. Photobio. A* **2012**, *247*, 24-29.

[36] P. Batat, M. Cantuel, G. Jonusauskas, L. Scarpantonio, A. Palma, D. F. O'Shea, N. D. McClenaghan, *J. Phys. Chem. A* **2011**, *115*, 14034-14039.

[37] W. Min, S. Lu, S. Chong, R. Roy, G. R. Holtom, X. S. Xie, *Nature* **2009**, *461*, 1105-1109.

[38] D. Escudero, *Acc. Chem. Res.* **2016**, *49*, 1816-1824.

[39] M. J. Hall, L. T. Allen, D. F. O'Shea, *Org. Biomol. Chem.* **2006**, *4*, 776-780.

10.1002/chem.202104072

WILEY-VCH

RESEARCH ARTICLE

For Table of Contents Only